MATRIX PENCIL METHOD INTEGRATION INTO STABILIZATION DIAGRAM FOR POLES IDENTIFICATION IN ROTORCRAFT AND POWERED-LIFT APPLICATIONS

Paolo Pivetta, paolo.pivetta@leonardocompany.com, Leonardo Helicopters (ITA)
Alberto A. Trezzini, albertoangelo.trezzini@leonardocompany.com, Leonardo Helicopters (ITA)
Marco Favale, marco.favale@leonardocompany.com, Leonardo Helicopters (ITA)
Cristian Lilliu, cristian.lilliu@leonardocompany.com, Leonardo Helicopters (ITA)
Attilio Colombo, attilio.colombo@leonardocompany.com, Leonardo Helicopters (ITA)

Abstract
The development of a safe and reliable VTOL aircraft is largely dependent on the availability of accurate and practical model of the system. Due to the complex dynamic behavior of rotorcraft and related subsystems, system identification based on flight data is essential in producing representative models. Traditional approaches, such as the polynomial based Prony method, are computationally expensive and sensitive to signal noise and disturbances. They also lack any indication of reliability and typically require time-consuming manual post-verification by a specialist.
Given the unique complexity of VTOL aircraft, associated poor signal to noise ratio, and presence of tonal disturbances in flight data, current system identification methods are not robust enough. In this paper, a comprehensive two-step method is presented to address the mentioned limitations of current techniques.
The proposed method is an output-only identification technique, based on time-domain analysis of the free decay response. Here, a modified Matrix Pencil (MP) method is coupled with the stabilization diagram to identify system poles. The main features of the method are the capability to assess simultaneously multiple time-histories in order to obtain a more comprehensive description of the system and, at the same time, a time saving analysis; the independence of tonal disturbances and noise; the generation of a qualitative measure of confidence on the results.
The algorithm was implemented in a software package, and extensive evaluation of the method was conducted using flight data. The results of the evaluation confirmed the capability of the method to detect poles within proximity of tonal disturbances. In addition, indicated an efficiency improvement of 70% in automatic system pole identification in high-noise signals when compared to MP techniques not used in conjunction with stabilization diagram.

1. ACRONYMS AND NOTATION

MASST	Modern Aeroservoelastic State Space Tools
MPE	Matrix Pencil Estimation method
SIMMPOLE	System Identification Method for Multi POLes Estimation
S/N	Signal Noise Ratio
SVD	Singular Value Decomposition
SWB	Symmetric Wing Bending
SWC	Symmetric Wing Chord
SWT	Symmetric Wing Torsion
σ	Singular Value
ζ	Damping Ratio

2. INTRODUCTION

System identification is a critical step in the development of a reliable VTOL aircraft. The complexity is determined by the aircraft modal characteristics and the environment in which flight data is recorded and analyzed. Typically, signal is disturbed by harmonics generated from rotors or systems like engines and gearboxes. Rotors harmonics are the most critical since they lie in a range of frequencies usually near to the investigated dynamics. This is also true for other special conditions like ground resonance test stability, in which the 1/rev is close to the lead-lag frequency. In addition, the presence of noise in terms of turbulence or gusts, undermines the accuracy and robustness of the identification. For

Presented at 45th European Rotorcraft Forum, Warsaw, Poland, 17-20 September, 2019

this reason, it is essential for the system identification method to be reliable and robust towards tonal disturbances and noise. It should also have to capability to assist the specialist identifying the relevant dynamics of the system, considering also the necessity to provide a result as quickly as possible when in telemetry. The method proposed in this paper is an output-only identification technique, based on time-domain analysis of the free decay response. The method combines the Matrix Pencil (MP) with the stabilization diagram in order to enhance the performances even in high noise level environments.

In this paper the two-steps identification technique will be described in detail in paragraph 3. In particular 3.3 will describe the extension of the basic MP method with the stabilization diagram and provide the method flowchart. Paragraph 3.5 will describe the multi-channel feature, which permits to provide an exhaustive result also in complex multi-modal environments as VTOL aircrafts. Section 4 will focus on the implementation of the method in the software SIMMPOLE and its features. Section 5 will report the validation of the method through a couple of meaningful test cases and a noise sensitivity assessment. Finally, further applications in the VTOL environment will be discussed in section 6.

3. METHOD THEORY

3.1. MPE

In order to identify the poles of a multiple degrees of freedom linear dynamic system with the MPE the time history of the system's free decay linear response is used. The system must be properly excited through one or more known inputs, which don't necessarily have to be measured since the MPE is here applied as an output-only method. From the moment in which the external excitation stops, the free decay linear response can be sampled. Therefore, a turbulent excitation cannot be used since it is impossible to identify an instant in which the excitation stops. A fundamental hypothesis ensuring that the method provides consistent results is that the sampled response can be considered as a free decay and no external unknown force should be applied to the system. This is since an undesired excitation during the free decay would cause an amplification of the response and then the signal would not be a free decay anymore.

Considering a general response signal (y) made of the free decay linear response of the system (x) and noise (n):

$$(1) \quad y(t) = x(t) + n(t) \qquad 0 \le t \le T$$

When sampled with *N* samples, the signal can be written as:

$$(2) \quad y(k) = x(k) + n(k) \qquad k = 0,1, \dots N-1$$

The method principle is the approximation of the time history by a sum of couples of complex exponentials. The system's response can be rewritten by the following:

$$(3) \quad y(k \cdot dt) \approx \sum_{i=1}^{M} R_i z_i^k + n(k \cdot dt) \qquad k = 0,1, \dots N-1$$

Where

$$(4) \quad z_i = e^{s_i dt} = e^{\left(-\alpha_i + j\omega_i^d\right)dt} = e^{\left(-\omega_i\zeta_i + j\omega_i\sqrt{1-\zeta_i^2}\right)dt} \qquad i = 1,2, \dots M$$

R_i are the complex amplitudes, s_i represent the poles of the system: ω_i are the angular frequencies and ζ_i are the damping ratios (c/c_{cr}). The elements $R_i z_i^k$ can be only complex conjugate couples. *M* is the order of the system

The aim then is to find the system's poles in terms of frequency and damping ratio. By determining also the complex amplitudes the system's response (x) can be reconstructed. This is helpful to check the quality of the estimation as it will be described later.

From the noiseless sampled signal $x(k)$ we can create the following rectangular Hankel matrix:

$$(5) \quad [X] = \begin{bmatrix} x(0) & x(1) & \cdots & x(L) \\ x(1) & x(2) & \cdots & x(L+1) \\ \vdots & \vdots & & \vdots \\ x(N-L-1) & x(N-L) & \cdots & x(N-1) \end{bmatrix}_{(N-L)\times(L+1)}$$

Where L is the pencil parameter, whose only limitation here is that it has to be smaller than $(N-1)$. The choice of its value will be discussed in the next paragraph.

From this matrix we can define two matrices $(N-L) \times L$ excluding the first and the last column of X:

$$(6) \quad \begin{aligned} [X_1]_{(N-L)\times(L)} &= [X(:,1\!:\!L)] \\ [X_2]_{(N-L)\times(L)} &= [X(:,2\!:\!L+1)] \end{aligned}$$

It is possible also to arbitrarily define a set of four matrices so that the following holds:

$$(7) \quad \begin{aligned} [X_1] &= [Z_1][R][Z_0][Z_2] \\ [X_2] &= [Z_1][R][Z_2] \\ [X_2] - \lambda[X_1] &= [Z_1][R]([Z_0] - \lambda[I])[Z_2] \end{aligned}$$

It can be demonstrated that M is the rank of the matrix pencil if $M \le L \le N - M$. And that the diagonal elements of the matrix $[Z_0]$ are the eigenvalues of the matrix pair $\{[X_2]; [X_1]\}$.

Presented at 45th European Rotorcraft Forum, Warsaw, Poland, 17-20 September, 2019

So, the problem of finding z_i can be set as the eigenvalue problem:

$$([X_1]^H[X_1])^{-1}[X_1]^H[X_2] - \lambda[I] \quad (8)$$

3.2. MPE Application to Noisy Signal

When analyzing a time history disturbed by noise $y(k)$, the same procedure to find the poles z_i can still be used, but in this case additional operations are required to ensure that the noise does not affect the results.

First, when defining the Hankel matrix $[Y]_{(N-L)\times(L+1)}$, the pencil parameter L is the first variable to be considered. For efficient noise filtering various sources ([3]) suggest choosing L as large as possible but limiting to the range $\left[\frac{N}{3}, \frac{N}{2}\right]$. For these reasons in these analyses it has been chosen equal to $\frac{N}{2}$.

After the creation of the Hankel matrix a fundamental step in order to filter out noise is to perform a singular value decomposition (SVD) of the matrix:

$$[Y] = [U][\Sigma][V]^H = [U]\begin{bmatrix} \sigma_1 & & \\ & \ddots & \\ & & \sigma_{L+1} \\ & & \end{bmatrix}[V]^H \quad (9)$$

Matrices $[U]_{(N-L)\times(N-L)}$ and $[V]_{(L+1)\times(L+1)}$ are complex unitary matrices made by a set of orthonormal eigenvectors of $[Y][Y]^H$ and $[Y]^H[Y]$, while $[\Sigma]_{(N-L)\times(L+1)}$ is a diagonal matrix that contains the singular values (σ_i) of $[Y]$. All of the singular values are real non-negative numbers and are ordered based on their relative magnitude. The firsts, larger singular values are the most representative of the analyzed system.

From the analysis of the singular values it is possible to determine, in first approximation, the order of the system (M).

In the favorable case of a very high signal to noise ratio (S/N) the order of the system is readily determined since the first M singular values are much larger than the following ones. In presence of a lower S/N instead, the distinction between the singular values that can be attributed to the real states of the system and the ones caused by the noise is more difficult to be appreciated. For this reason, in this application, the identification of M is done through two steps: first the singular values are normalized, then the derivative of the sorted and normalized singular values array is computed. The order of the system is determined as the array argument in correspondence of the maximum of the first derivative.

Then, It is possible to truncate the matrices $[\Sigma]_{(N-L)\times(L+1)}$ and $[V]_{(L+1)\times(L+1)}$ to the first M dominant singular values and related right singular vectors, obtaining the “filtered” matrices $[\Sigma']_{M\times M}$ and $[V']_{(L+1)\times M}$. It is possible to define:

$$\begin{aligned} [Y_1] &= [U][\Sigma'][V_1']^H \\ [Y_2] &= [U][\Sigma'][V_2']^H \end{aligned} \quad (10)$$

Where $[V_1']$ and $[V_2']$ are obtained by removing respectively the last and the first row from the matrix $[V']$.

As described in the previous paragraph, in order to find the poles z_i of the system, the following eigenvalues problem have to be solved:

$$[Y_1]^+[Y_2] - \lambda[I] \quad (11)$$

Which is equivalent to:

$$([V_1']^H)^+[V_2']^H - \lambda[I] \quad (12)$$

Once the poles z_i have been evaluated it is possible to find the complex amplitudes R_i through a least-squares problem:

$$\begin{bmatrix} y(0) \\ y(1) \\ \vdots \\ y(N-1) \end{bmatrix} = \begin{bmatrix} 1 & 1 & \cdots & 1 \\ z_1 & z_2 & \cdots & z_M \\ \vdots & \vdots & & \vdots \\ z_1^{N-1} & z_2^{N-1} & \cdots & z_M^{N-1} \end{bmatrix} \begin{bmatrix} R_1 \\ R_2 \\ \vdots \\ R_M \end{bmatrix} \quad (13)$$

Taking into account the definition of z_i and s_i:

$$\begin{aligned} z_i &= e^{s_i \cdot dt} \\ s_i &= -\omega_i\zeta_i \pm j\omega_i\sqrt{1-\zeta_i^2} \end{aligned} \quad (14)$$

It is possible to explicit the frequency and damping ratio of the calculated poles:

$$s_i = \frac{\ln(z_i)}{dt} \quad (15)$$

$$\begin{cases} f_i = \dfrac{\omega_i}{2\pi} = \dfrac{|s_i|}{2\pi} \\ \zeta_i = -\dfrac{Re(s_i)}{|s_i|} \end{cases} \quad (16)$$

3.3. Stabilization Diagram

The first noise-filtering method implemented in the basic MPE is the SVD and the related matrices truncation, which has been described in the previous paragraph. Although the effectiveness of this implementation is considerable, it is not sufficient to effectively determine the poles in presence of low S/N.

This is since an optimum choice of the parameter M depends on the noise level. The main effect of noise on the matrix of singular values $[\Sigma]$ is to increase the relative magnitude of the normalised singular values. As a matter of fact, if SVD is performed on a pure white noise, the singular values are homogeneous and smoothly

Presented at 45th European Rotorcraft Forum, Warsaw, Poland, 17-20 September, 2019

distributed. To reconstruct the original signal, the complete set of singular values must be considered since any of them is representative of the system.

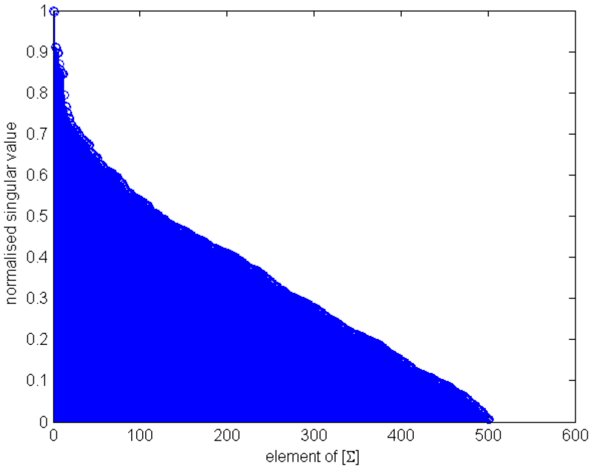

Figure 1. Normalised singular values array from a white noise time history.

For this reason, when calculating the derivative of the normalized singular values for a noisy signal, it is more challenging to identify the peak in the singular value derivative that gives the order of the system (M). It is highly probable to fail in determining the correct order of the system. Nevertheless, the highest peak of the derivative of singular values still provides a hint of how many poles are the most representative of the system.

The MPE poles evaluation is based on the selection of the correct order and provides M complex poles as a result. If the selection of M is not appropriate, part of the reconstructed poles will not possess a physical meaning because the method is introducing numerical artifacts while reconstructing the system properties.

To overcome this element of uncertainty on the correct order due to the noise, the concept of stabilization diagram has been exploited and applied to MPE. After SVD, the array $\underline{M}$ is created. Its elements are increasing values of the order, starting from M_{min} which is the order identified through the singular values analysis. The MPE analysis described above is then repeated on the same data set changing the order M at every iteration. For every iteration an array of poles $\underline{s}$ (dimensions $\times 1$) is evaluated. At the end of the iterations all the $\underline{s}$ arrays are clustered in a single matrix $[s]$ of dimensions $M_{max} \times length(\underline{M})$.

On this matrix of poles, a stability search is performed to identify the poles which recur the most across the iterations. As the order increases only the true poles of the system remain stable and recur at almost every iteration, while the others will scatter across the complex plane. The number of analyzed orders should be large enough to observe the stability of the poles that possess a physical meaning.

The stability of poles is checked both on the real and imaginary part (it is equivalent to checking on frequency and damping ratio) by setting a variability threshold of 15% on the real part and 1% on the imaginary part.

The stability search algorithm is made of the following main steps:

- From the matrix $[s]$ of complex poles are created two column arrays containing the real ($\underline{\mathrm{Re}}$) and imaginary parts ($\underline{\mathrm{Im}}$);
- The arrays are sorted by the real part array;
- Every element of the arrays is checked with respect to the following element to be simultaneously inside the variability range of the real and imaginary part:

$$(17) \qquad \begin{cases} \dfrac{\mathrm{Re_{i+1}} - \mathrm{Re_i}}{\mathrm{Re_i}} < 15\% \\ \dfrac{\mathrm{Im_{i+1}} - \mathrm{Im_i}}{\mathrm{Im_i}} < 1\% \end{cases} \qquad i = 1,2 \ldots N_p - 1$$

- All the elements that satisfy the previous conditions are grouped. For each group an overall check on the variability range is performed. In this case the reference values are the mean real and imaginary parts of each group. This is done to prevent the case in which the firsts and lasts values of each group are beyond the chosen threshold.
- Each group now identifies a pole ($\hat{s}_i$) constituted by the mean real part and the mean imaginary part of the group, whose repetitions in the stabilization diagram analysis are as many as the number of elements which form the group.

The output of the stability search algorithm is the set of poles identified by frequency, damping (alternatively imaginary and real part of the complex pole) and repetitions. Repetitions are the primary mean to discriminate between physical poles and those produced by noise and provide a quantitative accuracy of the result: the higher is the repetition of a pole, the more accurate and more reliable is the solution found. Repetitions are not indicated as an absolute value, but rather as a percentage of the number of iterations of the stabilization diagram. This allows an easier determination of the accuracy of the result.

In general, based on experience accrued on data analysis of thousands of instances, a good result is characterized by a repetition percentage around 75% and above, between 50% and 75% the poles

Presented at 45th European Rotorcraft Forum, Warsaw, Poland, 17-20 September, 2019

may be partially accurate but may be satisfactory for real time in flight monitoring, while values under 50% are normally considered unreliable.

In the diagram below the logical scheme of the MPE enhanced by the stabilization diagram algorithm is reported.

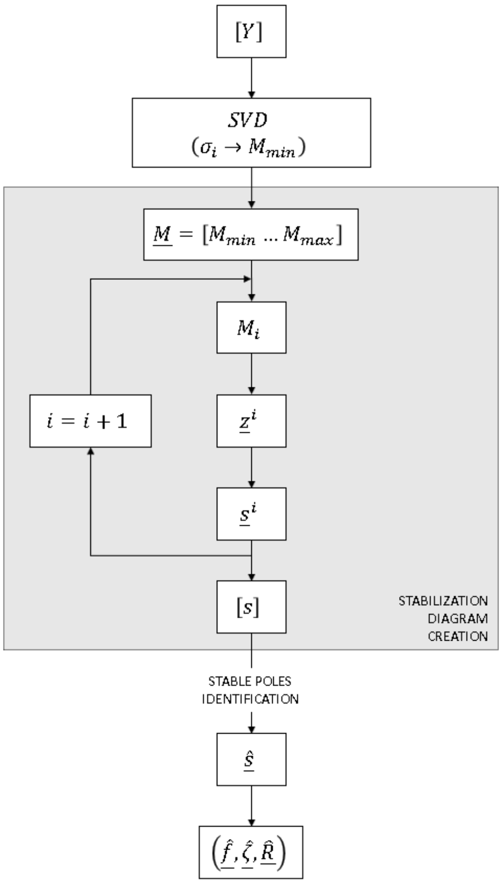

Figure 2. Method Flowchart

3.4. Time History Reconstruction

In addition to repetitions of the poles, another important mean to check the accuracy of the obtained results is the comparison of the original time history (y) with the reconstructed one (y_{rec}). The reconstruction error e_y is defined:

(18) $$e_y = y_{rec} - y$$

Where

(19) $$y_{rec} = \sum_i \widehat{R_i}\, e^{\widehat{s_i}\, dt}$$

The principle is that if the reconstructed system contains the complete set of relevant poles representative of the underlying system, then the difference between original and reconstructed time histories should be caused only by noise. Yet, sometimes the comparison does not provide a reliable insight on the result quality. As an example, when dealing with multiple poles that cause non-trivial time histories (beatings, apparent amplifications, etc.), the comparison in the time domain may provide spurious false negative due to negligible error in the relatives phase of the various system dynamics that causes non-negligible differences in the reconstruction.

In order to determine the reliability of the identification with even higher accuracy, autocorrelation and frequency domain techniques of the error may be used. In this application, FFT has been implemented since it was considered (and demonstrated by experience) suitable for the scope. By evaluating the FFT of the error it is possible to highlight the frequency content of the remainder of the original signal that has not been considered by the identified poles. Best possible result is a spectrum equivalent to a white noise input of low amplitude, since that would mean that no harmonics are missing from reconstructed time history and that error is minimum.

3.5. Extension to Multi-Channel Input

The input can be a single time history or multiple ones. When available it is recommended to use multiple inputs for the following reasons:

- Adding more constraints and comparing different types of sensors (e.g. accelerometers and strain gauges) improves the robustness of the solution;
- In case of multi-poles systems, data from different acquisitions can improve the identification of poles related to specific modal shapes that may be not captured by other sensors. For example, if sensor A is positioned in a node of a mode we are interested in, but sensor B is in an antinode, then using both sensors it is possible to catch that poles couple.

When using multi input, a matrix $[y]$ is created instead of a column array, in which each signal is a column. Each time history participates equally in the identification process, so it is important to select the signals with the best S/N in order to introduce more system information than errors:

(20) $$[y] = [\, \underline{y}_{(1)} \quad \underline{y}_{(2)} \quad \cdots \quad \underline{y}_{(N_y)} \,]$$

When creating the general Hankel matrix $[Y]$, the Hankel matrices from every time history are in the form $\left[Y_{(j)}\right]_{(N-L)\times L+1}$, so the overall matrix can be written as:

(21) $$[Y] = \begin{bmatrix} Y_{(1)} \\ \vdots \\ Y_{(N_y)} \end{bmatrix}_{N_y(N-L)\times(L+1)}$$

Presented at 45th European Rotorcraft Forum, Warsaw, Poland, 17-20 September, 2019

Every row of the final Hankel matrix is then an interval (of $L+1$ points) of one of the analyzed time histories. Since the dimensions of $[Y]$ are $N_y(N-L)\times(L+1)$ the number of singular values is $L+1$, independently from the number of time histories N_y.

4. SOFTWARE APPLICATION: SIMMPOLE

This method has been implemented in SIMMPOLE: a software developed in Matlab. The core of the software is the method described in the previous paragraph, but for more efficient analyses, in SIMMPOLE some additional features are implemented.

4.1. Normalization

It is possible to normalize the input data $[y]$. This action is intended mainly for cases in which input signals correspond to different types of measurements (such as accelerometers and strains gauges). When analyzing simultaneously different types of data, results are generated mainly by the channel with the greater amplitude. With normalization instead the different order of magnitude can be levelled and hence data can be compared more efficiently.

On the other hand, if data are homogenous, then the normalization may be even detrimental. During the normalization procedure, every time history is rescaled, therefore there is a potential risk to amplify noisy signals and reducing the weight of the clean ones. The risk of increasing the overall noise instead of adding system information is another reason to carefully choose the input data instead of selecting all the available ones. Here the dynamic analyst experience plays a relevant role.

4.2. Filters

In SIMMPOLE a set of filters is available: Butterworth or Chebyshev applied as low-pass, high-pass or band-pass. The use of filters can be useful to increase data S/N, but must be performed carefully. Depending on their order, filters add one or more couples of poles to the observed system. It is important then to apply filters in frequency ranges distant from the expected range of the system poles.

Efficient filters for helicopters are low-pass or stop-band in order to exclude the typical forcing harmonics of the aircraft like 2N/Rev or superiors.

4.3. Batch Analysis

In order to perform the analyses with greater speed and, at the same time, track better the analyzed cases, a batch mode of SIMMPOLE has been implemented.

In this mode each analysis must be detailed in an excel file in which the following must be specified:

- Input and reference data to be used;
- Normalization and/or filtering of the time histories;
- Time range of the input data to analyze;
- Solution selection filters like maximum frequency, maximum number and repetitions threshold for the output poles.

SIMMPOLE batch mode recalls each line and can perform a huge number of analyses limiting the required working time to 1-2 seconds per case. When available, in addition to the results of the enhanced MPE analyses, accessory flight data are provided also in order to relate poles positioning to certain aircraft conditions and parameters.

5. VALIDATION

To validate and demonstrate the performances of the algorithm implementation in SIMMPOLE, some test cases will be presented in the following paragraphs. All of them are performed on time histories generated analytically so that it is possible to measure the accuracy of the method.

5.1. Analytical Test Case

First test case is a damped sinusoid generated by a single couple of poles characterized by frequency $f = 5.5\ Hz$ and a damping ratio ζ equal to 4%. To investigate the effect of noise, a white noise signal has been added to the original damped sinusoid so that the resulting signal would present a S/N equal to 6.

Presented at 45th European Rotorcraft Forum, Warsaw, Poland, 17-20 September, 2019

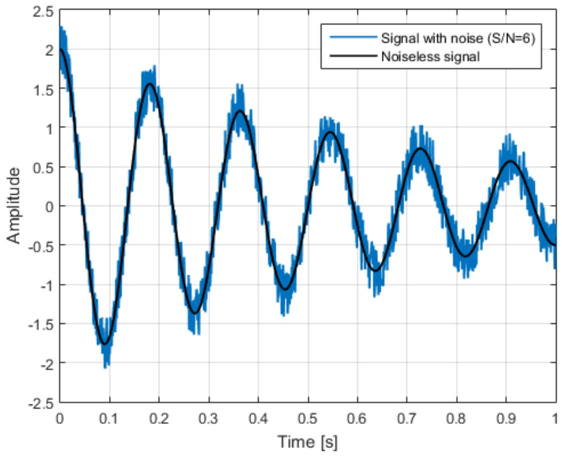

Figure 3. Analytical test case: original and noisy signals

The effect of noise can be highlighted, as previously discussed, in the determination of the order of the system. In Figure 4 and Figure 5 the singular values array and its derivative are shown.

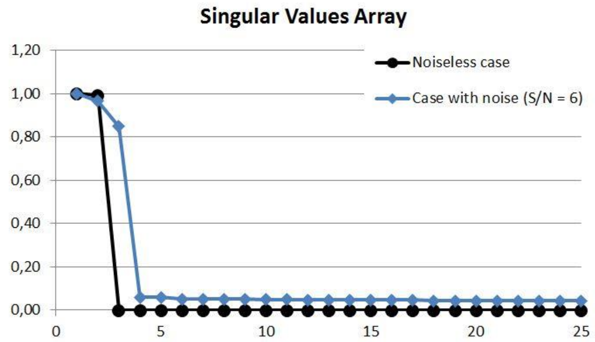

Figure 4. Singular values array

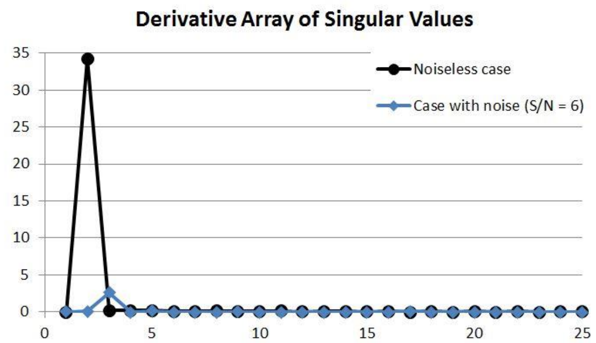

Figure 5. Derivative array of Singular Values

From these figures, which represent one of the easiest cases to reproduce, it is clear how noise flattens both indexes (singular values and derivative) and introduces an additional problem in identifying the order of the system, which gets more complicated as the number of system poles and noise level increase.

The identification of this test case has been performed in three different ways: analyzing the original noiseless time history and the noisy signal with basic MP, applying the extended method (Stabilization Diagram) to the noisy case. Results are shown in the following table. The extension of MP method with Stabilization Diagram is indicated with MPE.

	Frequency [Hz]	Damping Ratio [%]	Frequency Error [%]	Damping Ratio Error [%]
Analytical Solution	5,5	4%		
MP w/o noise	5,50	4,00%	0,0%	0,0%
MP w/ noise (S/N = 6)	5,47	3,37%	0,5%	15,8%
MPE w/ noise (S/N = 6)	5,50	4,06%	0,0%	-1,5%

Figure 6. Analytical test case results comparison

Basic MP is able to identify with precision the system characteristics when the time history is perfectly noiseless. The introduction of a disturb however generates a considerable error in terms of percentage. This inefficacy can be overcome using the extended method which permits to identify frequency and damping with a much more contained and acceptable error.

5.2. MASST Model Test Case

The second test case has been generated with MASST (Modern Aeroservoelastic State Space Tools), a piece of software for aeroelastic analysis developed in Matlab environment by Politecnico di Milano. MASST main feature is the possibility to integrate linear time invariant reduced subsystems models (such as airframe, rotors, drive train, etc.) of a fixed or rotary wing aircraft ([8],[9]).

The time histories employed for the validation of the algorithm have been generated with the AW609 MASST model. The overall model is made of a Nastran-based fuselage characterized by eight modes and modal damping derived from GVT results. Rotor is modeled in CamradII as a 14 multiblade DOFs including gimbal motion.

Figure 7. AW609 MASST Model

Presented at 45th European Rotorcraft Forum, Warsaw, Poland, 17-20 September, 2019

Turbulence conditions (S/N = 6) have been simulated through von Kármán win turbulence. A condition at Vh with a symmetric cyclic dwell excitation at f_1 has been used to excite the SWB mode and generate the second test case. Two channels corresponding to center wing accelerometers are used as inputs for this identification (see Figure 8).

The time range considered for the analysis is 2 s, starting 0.1 s after the end of the excitation.

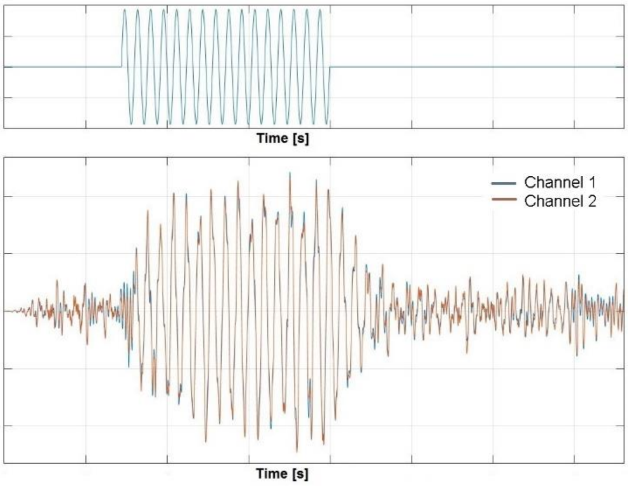

Figure 8. On the top window the reference excitation signal, while on the bottom are shown the two channels time histories generated by MASST

The result of identification with SIMMPOLE provides the following errors:

	Identification Error on SWB [%]
Frequency	-1.0%
Damping ratio	-2.6%

Figure 9. MASST model test case result errors

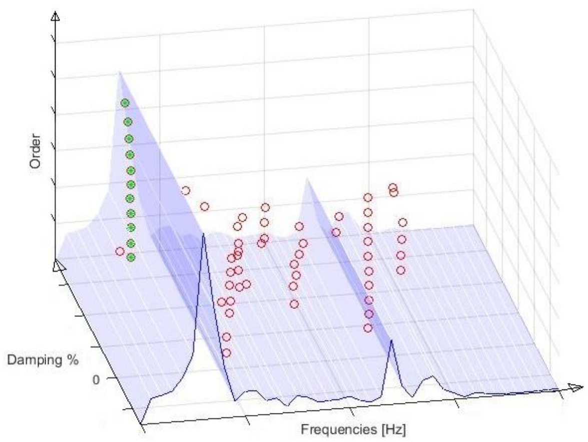

Figure 10. Stabilization diagram for MASST-generated test case

Figure 10 shows the stabilization diagram and the FFT of the original signal. It can be noted that the main pole (relative to SWB mode) is well identified at low frequency, while more poles are present at higher frequencies. Among those, many are generated by noise, while some are relative to the other modes of the system. Nevertheless, the dwell frequency f_1 is quite distant from the other mode frequencies and the excitation type is cannot stimulate a significant dynamic response of other modes. Observing Figure 11, the reconstruction of the time history is acceptable, as confirmed by the FFT of the residuals (Figure 12), which presents a quite uniform spectrum. This means that the reconstruction error is equivalent to noise in terms of frequency content, hence no significant harmonics have been missed.

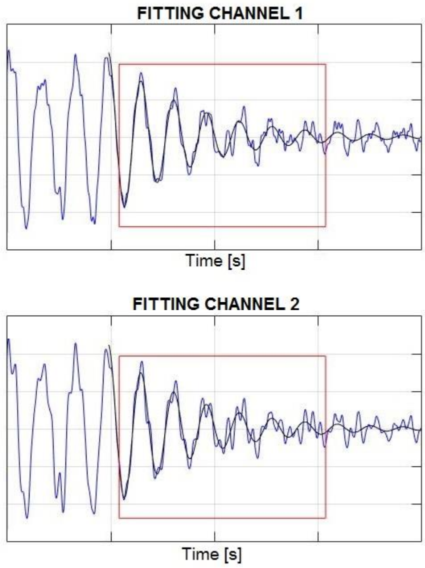

Figure 11. Original vs reconstructed time histories of the analyzed channels. The boxes show the actual time range used for the identification.

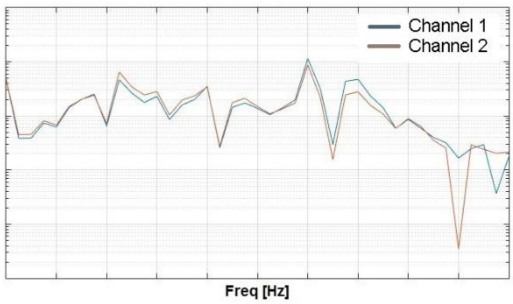

Figure 12. FFT of the residuals

5.3. Noise Sensitivity Assessment

In addition to previous test cases, a sensitivity on the accuracy and robustness of the identification depending on noise has been assessed. Time histories have been generated by the AW609 MASST Model described in the previous paragraph and three modes have been excited through dwells: SWB, SWT and SWC. Each of them has been modeled with four different levels of turbulence: 2.5%, 5%, 7.5% and 10% of the signal amplitude. Twenty record have been created for each condition, obtaining an overall of 240 cases, which have been analyzed with the SIMMPOLE batch feature. While processing data with batch mode, it might happen that a solution is not found if the boundary conditions are too restrictive. For this assessment, the percentage of found solutions is primarily dependent on noise intensity, and secondarily also on the aircraft mode.

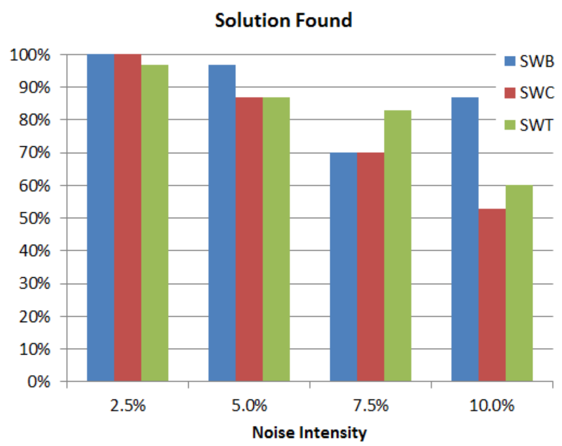

Figure 13. Percetage of found solution for each condition

In the following figures the distribution of resulting poles is shown only for the SWB case for sake of conciseness. Poles distributions relative to SWT and SWC mode are equivalent to those shown.

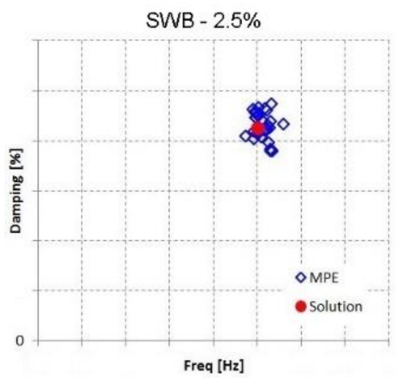

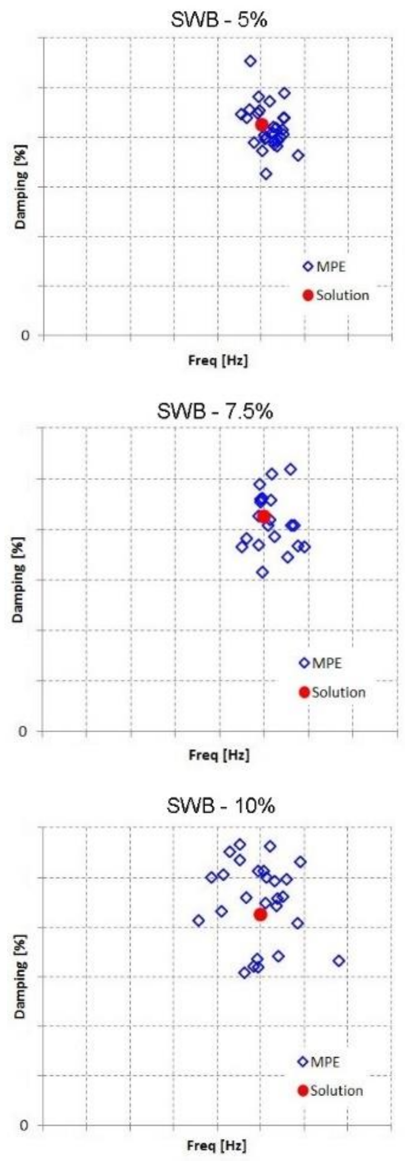

Figure 14. SWB mode identified poles distribution for four levels of noise

In the following tables the average errors on the identified poles are summarized for each condition in terms of frequency and damping ratio. An overall average error depending on noise level only has been calculated too. The trend is quite clear: average error tends to increase with noise level, as can be observed from previous figure too. Bigger errors are observed on damping, anyway, not exceeding 10% in this assessment.

Presented at 45th European Rotorcraft Forum, Warsaw, Poland, 17-20 September, 2019

	Frequency Error [%]			
Noise	2.5%	5%	7.5%	10%
SWB	0.2%	0.3%	0.3%	0.0%
SWC	0.1%	0.1%	0.3%	0.1%
SWT	0.1%	0.2%	0.2%	0.4%
Avg	0.1%	0.2%	0.3%	0.2%

	Damping Ratio Error [%]			
Noise	2.5%	5%	7.5%	10%
SWB	1.3%	1.2%	9.8%	6.1%
SWC	0.5%	1.3%	6.1%	7.6%
SWT	1.5%	1.2%	2.0%	2.6%
Avg	1.1%	1.2%	6.0%	5.4%

Figure 15. Average errors on identified poles

In addition to the average values, a boxplot of the errors on frequency and damping has been performed in order to describe its statistical distribution.

As far as frequency regards, the distribution of error is always limited between [-1.4%; 1.3%]. While for damping ratio the scatter is more obvious: the whiskers limits are [-34%; 33%], while the box limits are [-8%; 10%], hence at least 50% of the results has an error under 10%.

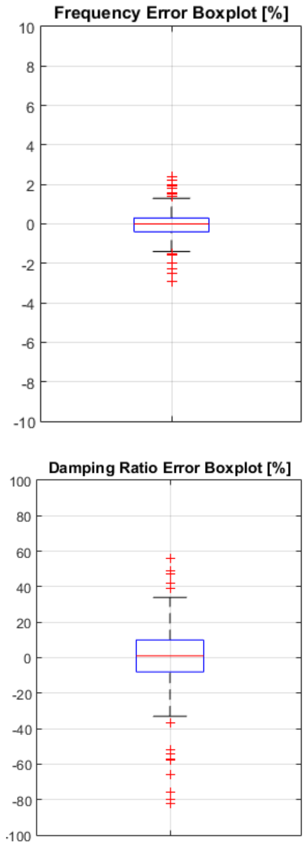

Figure 16. Error Boxplots for frequency and damping ratio results obtained with batch analysis on 240 cases

6. FURTHER APPLICATIONS

In addition to the flight conditions analyses which have been presented in the previous paragraph, this method can be applied to many other aircraft conditions. The only critical point is the availability of a free decay time history: every forcing not registered acting during the time window analyzed would be interpreted as an instability since the response of the system would be usually amplified by the excitation. Among many possible applications, two relevant ones are presented: Human External Cargo (HEC) and Ground Resonance (GR).

6.1. Human External Cargo

HEC is an equipment installed on helicopters intended for people transportation. It consists of a fixed length rope (up to 90 m) secured at one end to a barycentric hook, and at the other to the cargo. Since the cargo is human, an additional backup rope is installed in case of failure of the main rope attached to the aircraft belly. In case of failure the cargo would be subjected to a free fall until the backup rope enters tension and load is transferred to the backup hook, so that the whole system would start oscillating. In this case the excitation corresponds to the impulse derived from the tensioning of the backup rope. The main source of noise instead is the pendulum-related oscillations.

SIMMPOLE has been employed to analyze the flight test time histories of these events in order to describe the stiffness and damping properties of the system for various configurations of length of main and backup ropes and cargo weight. In the following figures the HEC scheme and a typical flight test record are shown.

Figure 17. Human External Cargo

Presented at 45th European Rotorcraft Forum, Warsaw, Poland, 17-20 September, 2019

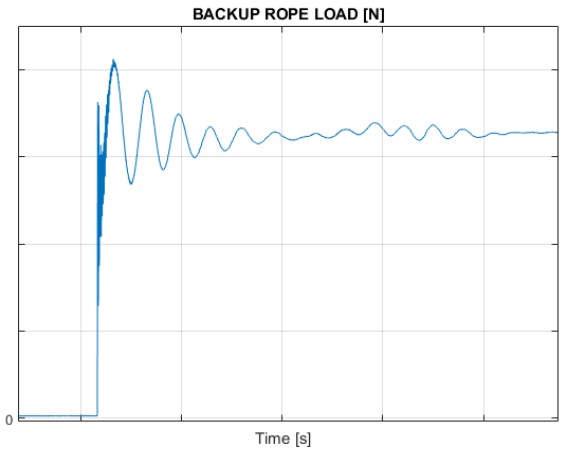

Figure 18. Example of HEC backup rope load time history

From the last figure, it can be observed that two types of disturb are present while backup rope is loaded. The first one is a high frequency disturb probably generated by the links between the ropes, while the second disturb, more evident after the first cycles is due to the pendulum oscillation of the HEC.

6.2. Ground Resonance Test

For ground resonance applications the method can be applied to investigate the damping of the system during the relative GR stability tests. Measuring the margin on stability through a method like the one presented on this paper, instead of just verifying the stability of the aircraft for each condition, would give much more insight to the specialists.

The aim of the test is the verification of stability when the aircraft is forced through circular motion imposed on cyclic commands at certain frequencies. Motion can be induced by a software-controlled actuation or directly by the pilot. In the example reported below the cyclic motion is produced by the pilot. The identification of the poles of the system and their damping is performed on the aircraft body roll rate signal.

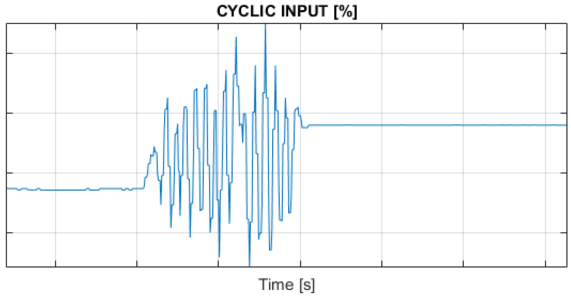

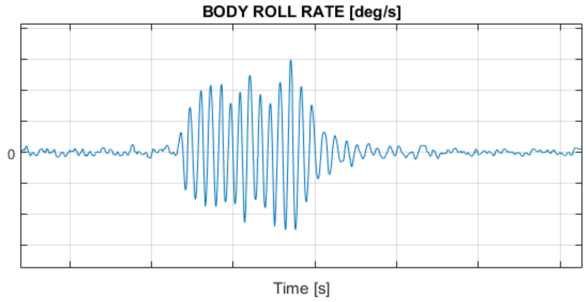

Figure 19. Ground Resonance typical test data

7. CONCLUSIONS

Considering the unique complexity of VTOL aircraft, the associated poor signal to noise ratio, and the presence of tonal disturbances in flight data, the implementation in SIMMPOLE of Matrix Pencil method extended with Stabilization Diagram has been shown to provide reliable and accurate results. The multi-channel input permits to evaluate at the same time the complex modal responses of the aircraft. Stabilization Diagram and the repetition-based method for selecting the more representative poles of the system give the specialist a good confidence of the accuracy of the results. The efficacy of the method has been validated with both simple analytical and more VTOL representative test cases created with MASST. An assessment on noise sensitivity has been presented, showing an acceptable scatter distribution of error even in high noise signals. Finally, among the multitude of possible applications, the HEC dynamic response analysis and the Ground Resonance Test Stability have been described.

Presented at 45th European Rotorcraft Forum, Warsaw, Poland, 17-20 September, 2019

8. REFERENCES

[1] R. Kumaresan, D.W. Tufts - “Estimating the Parameters of Exponentially Damped Sinusoids and Pole-Zero Modelling in Noise”

[2] T.K. Sarkar, O. Pereira - “Using the Matrix Pencil Method to Estimate the Parameters of a Sum of Complex Exponentials”

[3] Y. Hua, T.K. Sarkar - “On SVD for Estimating Generalized Eigenvalues of Singular Matrix Pencil in Noise”

[4] Y. Hua, T.K. Sarkar - “Matrix Pencil Method for Estimating Parameters of Exponentially Damped/Undamped Sinusoids in Noise”

[5] Y. Hua, T.K. Sarkar - “Perturbation Analysis of TK Method for Harmonic Retrieval Problems”

[6] R. Mahmoudvand, M. Zokaei - “On the singular values of the Hankel matrix with application in singular spectrum analysis”

[7] M. Favale, D. Prederi, A. A. Trezzini - “Prediction of AW609 Rotor Loads by Means of Neural Networks”

[8] P. Masarati, V. Muscarello, and G. Quaranta. Linearized aeroservoelastic analysis of rotary-wing aircraft. In 36th European Rotorcraft Forum, pages 099.1-10, Paris, France, September 7-9, 2010”

[9] P. Masarati, V. Muscarello, G. Quaranta, A. Locatelli, D. Mangone, L. Riviello, and L. Viganò. An integrated environment for helicopter aeroservoelastic analysis: the ground resonance case. In 37th European Rotorcraft Forum, pages 177.1–12, Gallarate, Italy, September 13-15 2011

Presented at 45th European Rotorcraft Forum, Warsaw, Poland, 17-20 September, 2019